

RSC Advances



This is an *Accepted Manuscript*, which has been through the Royal Society of Chemistry peer review process and has been accepted for publication.

Accepted Manuscripts are published online shortly after acceptance, before technical editing, formatting and proof reading. Using this free service, authors can make their results available to the community, in citable form, before we publish the edited article. This *Accepted Manuscript* will be replaced by the edited, formatted and paginated article as soon as this is available.

You can find more information about *Accepted Manuscripts* in the [Information for Authors](#).

Please note that technical editing may introduce minor changes to the text and/or graphics, which may alter content. The journal's standard [Terms & Conditions](#) and the [Ethical guidelines](#) still apply. In no event shall the Royal Society of Chemistry be held responsible for any errors or omissions in this *Accepted Manuscript* or any consequences arising from the use of any information it contains.

Amorphous Barium titanate thin film improves the light trapping in Si solar cells

A. K. Sharma^{1,2}, B. Geetha Priyadarshini^{1,3,*}, B. R. Mehta¹, Dinesh Kumar⁴

¹Thin Film Laboratory, Department of Physics, Indian Institute of Technology Delhi, India

²National Centre for Photovoltaic Research & Education, Indian Institute of Technology Bombay, India

³Nanotech Research Innovation & Incubation Centre, PSG Institute of Advanced Studies, Coimbatore, Tamil Nadu, India

⁴TATA Power Solar System Limited, Bangalore, India

* Corresponding author details

Dr. B. Geetha Priyadarshini

Assistant Professor,

Nanotech Research Innovation & Incubation Centre

PSG Institute of Advanced Studies

Peelamedu

Coimbatore- 641004, Tamil Nadu, INDIA

Email: bgp@psgias.ac.in (or) geethapriyadarshini@gmail.com

Mobile no.: +91 98438 21434

Tel: +91-422-434 4000, Ext: 4193

Fax: +91-422-257-3833

Amorphous Barium titanate thin film improves the light trapping in Si solar cells

A. K. Sharma^{1,2}, B. Geetha Priyadarshini^{1,3,*}, B. R. Mehta¹, Dinesh Kumar⁴

¹Thin Film Laboratory, Department of Physics, Indian Institute of Technology Delhi, India

²National Centre for Photovoltaic Research & Education, Indian Institute of Technology Bombay, India

³Nanotech Research Innovation & Incubation Centre, PSG Institute of Advanced Studies, Coimbatore, Tamil Nadu, India

⁴TATA Power Solar System Limited, Bangalore, India

Abstract

A new anti-reflection coating based on amorphous barium titanate (*a*-BTO) was developed using RF magnetron sputtering technique. Systematic studies on the structural and optical properties were carried on *a*-BTO thin films deposited on polished Si and textured Si substrates. In the visible range of solar spectrum, the refractive index was found to be 2.02–1.91 with high transmittance of greater than 85 %. Maximum reduction in the reflectance for *a*-BTO on polished Si and texture Si substrates was found to be 100 % (at 550 nm) to 85 % (at 400 nm), respectively. Further, improvement in cell efficiency of Si solar cell with *a*-BTO anti-reflection coating was found to increase from 9.3 % to 10 % with improvement in overall performance parameters such as short circuit density (J_{sc}), open circuit voltage (V_{oc}) and fill factor (FF). These results indicates that *a*-BTO thin film deposited using RF magnetron sputtering can be used as alternative anti-reflection coatings for Si based photovoltaic cells.

Keywords: *Light trapping, Anti-reflection coating, amorphous barium titanate, Si solar cell.*

1. Introduction

Barium titanate (BTO) is among the most extensively studied systems in perovskite class of materials. During cooling from high temperatures, BTO transforms from highly symmetric paraelectric cubic phase to slightly distorted ferroelectric structures with tetragonal, orthorhombic and rhombohedral symmetries at low-temperature [1]. Due to this phase transformation, BTO in bulk form, multi-layers, thin films and nanostructures shares variety of applications possessing exceptional dielectric, ferroelectric and piezoelectric properties [2-6].

Over the years, anomalous high photovoltages are observed in BTO which show potential for photovoltaic (PV) associated routes of energy generation through various conduction mechanisms. The photovoltaic effect in bulk and single crystal BTO was found to depend on the chemical composition, and grain size [7]. One of the early reports by Chynoweth revealed the presence of space charge-fields and potential variations across the crystals are responsible for associated photovoltaic effect in single crystal BTO [8]. High photovoltage resulted from the integration of small photovoltage across spontaneously polarized individual BTO grains [9]. Recently, Yang *et al.* [10] reported that the photovoltages are significantly higher than the bandgap of ferroelectric materials and the electric-field control over domain structure allows the photovoltaic effect to be reversed in polarity or when turned off. Cudney *et al.* observed generation of photogalvanic current at least two trap levels with two different strengths when the BTO crystal was illuminated by a spatially periodic light intensity pattern [11]. Xing *et al.* stated the reasons for large generation of photovoltage in BTO/Si heterojunction structure due to the low oxygen content and migration of oxygen vacancies leading to better conductivity [12]. Shift current is yet another dominant mechanism in bulk BTO as photocurrent does not only depend on the magnitude of material polarization, but also on electronic states with delocalized, covalent

bonding that is highly asymmetric along the current direction [13]. However, nanometer-sized BTO glass has wider transmittance window 250 nm – 11,000 nm and high refractive index ~ 2.15 which offers lower reflectance to the Si based photovoltaic devices [14]. Amorphous BTO thin films of 140 nm thick deposited using metalorganic chemical vapor deposition was reported to show high optical transmittance of 80 % with optical band gap of 4.71 eV in the visible wavelength range [15].

Light trapping is essential in order to achieve complete absorption of light in the Si solar cell. A commercial crystalline Silicon (c-Si) solar cell has 180 μm thickness with typical feature size of the texturing is in the range of 5–10 μm [16]. At the front side, they are covered with a pyramidal light-trapping texture coated with an 80-nm-thick Si_3N_4 antireflection layer [17]. Antireflection coating (ARC) enhances the absorption of photons through reduction in reflection thereby increasing the short circuit current density (J_{sc}) that translates into increase in solar cell efficiency. Ideal broadband anti-reflection requires complete removal of impedance mismatch that is possible when a dispersive, graded refractive index medium is used as impedance matching layer [18].

In this paper, we investigate the potential of *a*-BTO thin film coatings for light trapping in Si solar cells which could be an alternative for existing anti-reflection coating like Si_3N_4 , TiO_2 and MgF_2 etc. in near future. Therefore, the present study focuses on the development of *a*-BTO thin-films on polished and textured Si substrate with enhanced antireflection properties for improving Si solar cell performance by efficiently trapping visible light. The vital physical properties required for antireflection coating such as refractive index, and transmittance was evaluated for *a*-BTO thin film. The performance improvement in conventional monocrystalline silicon n^+ -p diffused junction solar cell for *a*-BTO coating is also discussed in detail.

2. Experimental details

2.1 Synthesis and characterization of antireflection BTO thin films

In this study BTO thin-films were deposited on the quartz glass, polished Si (*n* type and *p* type), textured Si and bare Si solar cells using rf-magnetron sputtering of BaTiO₃ target (99.99% purity). The deposition conditions are tabulated in Table 1.

The structural properties of BTO thin films were investigated using glancing incidence X-ray diffraction (GIXRD) and high-resolution transmission electron microscopy (HRTEM). The optical constants (*n*, *k*) and thickness (*t*) of thin-films was estimated using the M-2000F ellipsometer (J. A. Woollam Co., Inc). The reflectance and transmittance of barium titanate thin films deposited on different substrates was carried out using UV/Vis spectrophotometer (Perkin–Elmer Lambda 35) with an integrating sphere detector.

2.2 Solar cell fabrication and characterization

Boron doped CZ Si wafers of size 125 x 125 mm with thickness 200±10 μm and bulk resistivity in the range of 0.5-3 Ω-cm were used as the starting material for the solar cell fabrication. Solar cells were fabricated by the conventional silicon solar cell process with screen print technology. The saw damages and the residual contamination were removed by alkaline chemicals (NaOH, 40% vol./vol. at 80°C for 30 sec) followed by alkaline texturization (NaOH, 4% vol./vol., 85°C for 15 min). Consecutively, P-diffusion was carried out by using POCl₃ in a tube furnace. The diffusion was carried out at 880°C for 40 min to form a shallow junction (~0.3 micron junction depth). The phosphosilicate glass formed during diffusion process was removed in buffered HF (10% HF for 2 min) followed by plasma based edge isolation. The front and back contacts were made by using conventional screen print technology and simultaneously co-fired

to realize the ohmic contacts on the front surface as well as aluminum (Al) back surface field (BSF) on the back surface.

In order to evaluate the solar cell performance, the measurements were carried out with (test cell) and without (control cell) *a*-BTO coating on monocrystalline Si solar cells under one sun (100 mW/cm^2) using standard solar spectrum AM 1.5G. The performance parameters such as short circuit current density (J_{sc}), open circuit voltage (V_{oc}), fill factor (FF), series resistance (R_s) and shunt resistance (R_{sh}) were calculated from illuminated current density-voltage ($J-V$) characteristics. Also, solar cell collection efficiency in 400 - 1100 nm wavelength range was obtained with internal quantum efficiency (IQE) *i.e.* incident photon to converted electron ratio ($IPCE$) measurement.

3. Results and discussion

3.1 Structural properties

The structural characterization of sputtered BTO thin-films was done using x-ray diffraction (XRD) at glancing angle 0.5° . Fig. 1 shows the GIXRD pattern of as-deposited BTO thin-films deposited on Si substrate held at 500°C and with different Ar to O_2 ratios. There is no distinct peak signifying the amorphous phase formation due to relatively high deposition temperature of 500°C at which crystallization is likely to take place. Crystalline peaks of BaTi_2O_5 emerge in the amorphous background at $2\theta=25^\circ$ and very low intensity peaks of BaTiO_3 co-exists with the BaTi_2O_5 phase at higher O_2 flow rates. Presence of BaTiO_3 peaks in XRD profiles indicates that increase in O_2 flow rate during deposition favors nucleation of BaTiO_3 crystals in deposited thin films. When Ar to O_2 ratio was increased to 16:4, co-existence of BaTiO_3 and BaTi_2O_5 phases was observed. For this particular sample, refractive indices were calculated to be 2.42 and 2.15, respectively which might play a major role in minimising the reflection losses. Therefore, for the

present study on light trapping, BTO thin films deposited at Ar to O₂ gas ratio of 16:4 is chosen. Subsequently, BTO films with Ar: O₂ ratio of 16:4 sccm were deposited at room temperature (30 °C) to obtain amorphous phase on different substrates.

Figure 2 (a) shows the GIXRD patterns for BTO thin films deposited on different Si substrates such as p-Si, n-Si, textured Si and multi-crystalline Si. BTO thin films were predominantly amorphous around 2θ ranging from 25°-30° when deposited at room temperature which is desired for the present work. It is important to point out here, that at present it is difficult to comment on the formation of single phase *a*-BaTiO₃ or *a*-BaTi₂O₅ or both (*a*-BaTiO₃ and *a*-BaTi₂O₅) in the as-deposited films on different substrates. But it is certain from the XRD profile that the film structure is comprised of both the amorphous and nanocrystals of barium titanate with a broad peak centered at $2\theta=55^\circ$.

Fig. 2(b) shows HRTEM image and corresponding selected area electron diffraction pattern (SAED) consists of broad diffused ring without the presence of bright spots confirming the amorphous nature of BTO film. Despite the presence of amorphous BTO and nanocrystal BTO phase revealed by XRD analysis, a single diffused ring corresponding to glassy phase is obtained possibly due to similar *d*-spacing of BaTiO₃ and BaTi₂O₅.

Figure 2(c) is a digital photograph of sputtered *a*-BTO thin-films on textured (T_x) and polished (P) silicon substrates showing dark bluish colored coatings.

3.2 Optical properties

Major inference can be drawn on anti-reflection properties of the developed coatings by measuring refractive index, transmittance and reflectance values. Ellipsometric studies on

broadband, omnidirectionality, and polarization-insensitivity of antireflection coatings were examined systematically and further supported by UV-Vis spectrophotometric studies.

Fig. 3 (a) shows the refractive index (n), extinction coefficient (k) and real & imaginary parts of the dielectric function (e_1 , e_2) of deposited amorphous BTO thin films. The n value was found to be 2.02 at 400 nm and decreased to 1.89 at 1000 nm and varied from 1.98 -1.92 in the range 450 – 650 nm where maximum photon flux in the entire solar spectrum is available for energy conversion. These values of n agree with the requirement for ideal conditions of silicon solar cell based module [19]. The extinction coefficient (k) value found to be 0.009 at 400 nm and increased to a maximum value of 0.015 at 380 nm and then decreased to 0.000 at 1000 nm. In addition, e_1 decreased from its highest value 4.01 (at 400 nm) to 3.58 (at 1000 nm), whereas e_2 decreased from maximum value of 0.062 (at 486 nm) to a minimum value of 0.00 (at 1000 nm). The loss factor e_2/e_1 shows maximum dielectric loss in the 400 - 700 nm and almost zero loss beyond 750 nm. This observation emphasize that the visible portion holds greater dielectric loss in comparison to near infrared radiation of the spectrum signifying the potential of a -BTO layer as the anti-reflection coating in the maximum photon flux available in the solar spectrum.

To achieve an optimal anti-reflection effect resulting in zero net reflection in the spectral range of interest 450 – 650 nm, the amplitudes of the reflected beam at the air-coating interface and coating-substrate interface has to be equal and exactly one-half wave (180°) out of phase, resulting in destructive interference. The first condition can be met when refractive index of the coating (n) equals to the square root of the product of the refractive indices of substrate (n_s) and medium (n_o) expressed by eqn. 1 [20]:

$$n = \sqrt{n_s n_o} \text{-----(1)}$$

The second condition is that the optical thickness of the ARC layer must be close to a quarter of the wavelength at which zero reflectance should occur (*i.e.*, the reflected wave must be out of phase by π). This condition is expressed by eqn. 2:

$$n t = \frac{\lambda_{min}}{4} \text{----- (2)}$$

where t is the thickness of the ARC layer and λ_{min} is the wavelength at which the reflectance becomes minimum [21]. In the present study, the optimal thickness of *a*-BTO ARC layer was calculated to be ~70 nm for minimum reflection at wavelength of 550 nm and refractive index of 1.95.

Fig. 3 (b) shows the percentage reduction in the transmittance for *a*-BTO coated quartz substrate and reflectance for *a*-BTO antireflection coating on polished Si and textured Si substrates as function of the wavelength. The transmittance value 85 - 95 % in the wavelength range 400 - 1100 nm shows acceptance of *a*-BTO coating as a wide transmission window layer for the solar cell application. Recently, Masuno *et al.* reported wide transmission range in bulk counterpart of BTO glass in the wavelength range of 370 nm to 7.7 μm [22]. The measured transmittance values ensure the merit of transparency for the proposed *a*-BTO antireflection coating for Si solar cells. The relative reduction in the reflectance shown in fig. 3 (b) emphasize that the reflectance values are reduced for the entire wavelength range corresponds to the reflectance values for the bare substrates (not shown here). For *a*- BTO coated polished Si substrate, zero reflectance was observed at 550 nm, which depict that 100 % relative reduction in reflectance values of bare substrate. However, for *a*-BTO coated textured Si substrate, the minimum reflectance was found at 400 nm value and shows as 85 % relative reduction in pristine reflectance. The observed shift in wavelength value for minimum reflectance in polished Si (at

550 nm) and textured Si (at 400 nm) is possibly due the multiple reflection phenomenon taking place at the interface of *a*-BTO coating and textured Si substrate.

Typically, the surface of solar cell is textured in order to avoid photon loss due to multiple reflections. Therefore, in present study the solar cell surface assumed to be similar to the of textured Si surface as described in the experimental section.

3.3 Solar cell performance

Fig. 4 (a) shows the illuminated I-V characteristics and Table 2 illustrate the performance parameters of control and test Si solar cell. It is worth to mention here that the *a*-BTO coating was applied on the textured Si substrate. It was found that the J_{sc} increased by 1.41 mA/cm² and enhancement in V_{oc} was found to be 0.16 mV, respective to enhancement in current density. Further FF was found to increase by 1.60 % along with improvement in resistive losses *i.e.* increase in R_{sh} and R_s values by 22.81 Ω and 0.07 Ω , respectively. Therefore, the overall power conversion efficiency was improved by 7.5 %.

Fig. 4 (b) shows the internal quantum efficiency (IQE) plots for control and test cell that measures the incident photon to converted electron ratio. It is evident from IQE plot that the photon to electron ratio was improved for the absorption wavelength range 400 – 1100 nm due to the reduced reflectance for *a*-BTO coating, as previously described. For 400 - 500 nm spectral range, the relative reduction in reflectance was found to be ~ 80 % whereas improvement in IQE was 16 %. This is because of poor collection of photogenerated carriers, generated in 300 nm thick heavily doped n⁺ emitter region owing to high absorption coefficient (10⁵ cm⁻¹) of Si. Carrier recombination activity on front surface and heavily doped emitter region of diffused n⁺-p junction Si solar cell affects not only open-circuit voltage (V_{oc}) and the fill factor (FF) but also the short-circuit density (J_{sc}) very significantly and can be controlled through surface passivation

[23]. The inadequate improvement in IQE for spectral range 400–500 nm indicates less effective surface passivation capability of *a*-BTO coating. Hence with these observations, our future challenge is to improve the surface passivation with *a*-BTO coating adjunct to retaining the anti-reflection properties

4. Conclusion

A novel coating based on amorphous barium titanate thin films was developed using RF magnetron sputtering at room temperature. The refractive index values in the range 2.02 -1.91 and transmittance greater than 85 % in visible region range shows remarkable light trapping properties suitable as ARC layer for Si based photovoltaic solar cells. After coating with ~ 70 nm thick *a*-BTO thin film, nearly 100 % reduction in the reflectance value was observed for polished Si substrate at wavelength 550 nm and 85% for textured Si substrate at 400 nm. The improvement in the performance of Si solar cell with developed anti-reflection coating was also observed as cell efficiency increased from 9.3 % to 10 %. However, extensive studies are required on surface passivation behavior of *a*-BTO coating for solar cell in order to make this coating more beneficial to Si based PV devices.

References

- [1]. G. H. Kwei, A. C. Lawson, S. J. L. Billinge, S. W. Cheong, *J. Phys. Chem.*, 1993, **97** (10), 2368–2377.
- [2]. J. P. Ball, B. A. Mound, J. C. Nino, J. B. Allen, *J. Biomed. Mater. Res. A.*, 2014, **102** (7), 2089-95.
- [3]. E. Farrokh Takin, G. Ciofani, G.L. Puleo, G. de Vito, C. Filippeschi, B. Mazzolai, V. Piazza, V. Mattoli, *Int J Nanomedicine*. 2013, **8**, 2319-31.
- [4]. J.Y. Kim, H. Kim, T.Y. Kim, S. Yu, J. W. Suk, T. Jeong, S. Song, M. J. Bae, I. Han, D. Jung, S. H. Park, *J. Mater. Chem. C*, 2013, **1**, 5078-5083.
- [5]. N. Joseph, S. K. Singh, R.K. Sirugudu, V. R. K. Murthy, S. Ananthakumar, M. T. Sebastian, *Mater. Res. Bull.* 2013 48 (4), 1681-1687.
- [6]. R. Guo, L. You, Y. Zhou, Z.S. Lim, X. Zou, L. Chen, R. Ramesh, J. Wang, *Nat. Commun.*, 2013 **1990**, 4.
- [7]. W. Käppler and G. Arlt, *Phys. Stat. Sol.(a)*, 1981, **63**, 475–480.
- [8]. A. G. Chynoweth, *Phys. Rev.*, 1956, **102**, 705-714.
- [9]. P. S. Broady, *J. Solid State Chem.*, 1975, **12** (3-4), 193-200.
- [10]. S. Y. Yang, J. Seidel, S. J. Byrnes, P. Shafer, C.H. Yang, M. D. Rossell, P. Yu, Y. H. Chu, J. F. Scott, J. W. Ager, L. W. Martin, R. Ramesh, *Nat. Nanotechnol.* 2010, **5**, 143 - 147.
- [11]. R. C. Cudney, R. M. Pierce, G. D. Bacher, D. Mahgerefteh, A. Funicello, J. Feinberg, Proceedings of the *Conference on Lasers and Electro-Optics*, Anaheim, CA, USA, 1992, **12**.
- [12]. J. Xing, K. J. Jin, H. Lu, M. He, G. Liu, J. Qiu, G. Yang, *Appl. Phys. Lett.*, 2008, **92** (7), 071113-071113.
- [13]. S. M. Young, A.M. Rappe, *Phys. Rev. Lett.* 2012, **109**, 116601-116605.
- [14]. J. Li, G. Ba, P. Hu, J. Yang, Y. Chen, W. Pan, J. Yu, *J. Mater. Chem.*, 2012, **22**, 9450-9454.
- [15]. Y. S. Yoon, Y. K. Yoon, S.S. Yom, *Jpn. J. Appl. Phys.*, 1994, **33** 6663.
- [16]. M. A. Green, *Solar Cells: Operating Principles, Technology and System Applications*. Englewood Cliffs, NJ: Prentice-Hall, 1998.
- [17]. W. H. Southwell, *J. Opt. Soc. Amer.*, 1991, **8**, 549–553.

- [18]. K. H. Kim, Q. H. Park, *Sci Rep.*, 2013, **3**, 1062.
- [19]. B. Sopori, *J. Electronic Mat.*, 2003, **32** (10), 1034-1042.
- [20]. J. T. Cox and G. Hass, *Physics of Thin Films*, eds. G. Hass and R. E. Thun (Academic Press, New York, 1968), 1968, **2**, p.239
- [21]. L.N Hadley, Dennison DM. *J. Opt. Soc. Am.*, 1947, **37**, 451–465,
- [22]. A. Masuno, H. Inoue, J. Yu, Y. Arai, *J. Appl. Phy.*, 2010, **108** (6), 063520.
- [23]. A. K. Sharma, S. K. Agarwal, S. N. Singh, *Sol. Energy. Mater. Sol Cells*, 2007, **91**(15), 1515-1520.

Tables

Table 1: Deposition conditions of barium titanate thin-films.

Specification	Particulars
Base pressure (Torr)	1.5×10^{-5}
Deposition pressure (mTorr)	7.5
RF power (W)	100
Ar:O ₂ ratio (sccm)	20:0, 16:4, 10:10 and 0:20
Deposition temperature (°C)	30, 500
Deposition time (sec)	300

Table 2: PV performance parameter of control and Test solar cell

Parameter	Control cell	Test cell
Short circuit current density J_{sc} (mA/cm ²)	28.12	29.53
Open circuit voltage V_{oc} (mV)	558.00	558.16
Fill factor FF (%)	59.24	60.84
Efficiency (%)	9.30	10.00
Shunt resistance R_{sh} (Ω -cm ²)	278.26	301.07
Series resistance R_s (Ω -cm ²)	1.06	0.99

Figure 1

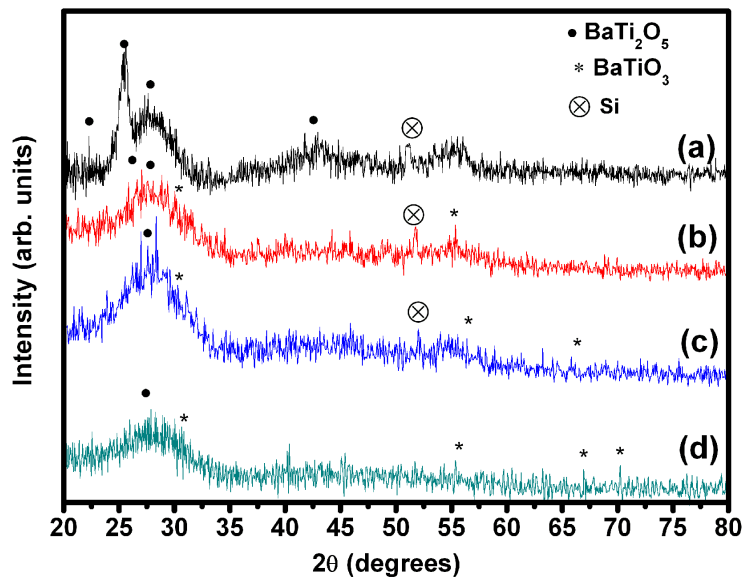


Figure 1: GIXRD pattern BTO thin films deposited at 500 °C on Si substrate with Ar:O₂ gas ratios of (a) 20:0 sccm, (b) 16:4 sccm, (c) 10:10 sccm and (d) 0:20 sccm.

Figure 2

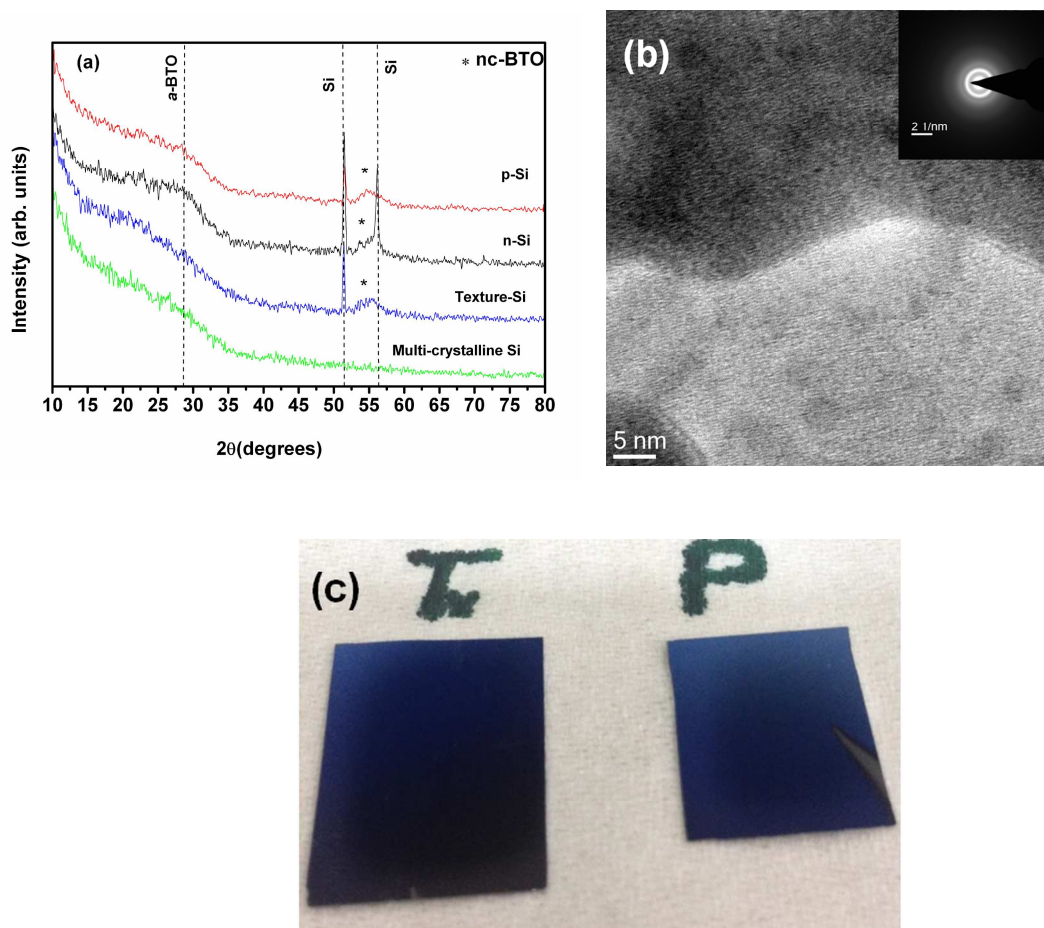


Figure 2: (a) GIXRD pattern of BTO thin films with Ar: O₂ ratio of 16:4 deposited at room temperature on different substrates; (b) TEM image with SAED inset of amorphous BTO thin film; (c) Digital photograph of dark bluish coating on textured and polished Si substrates.

Figure 3

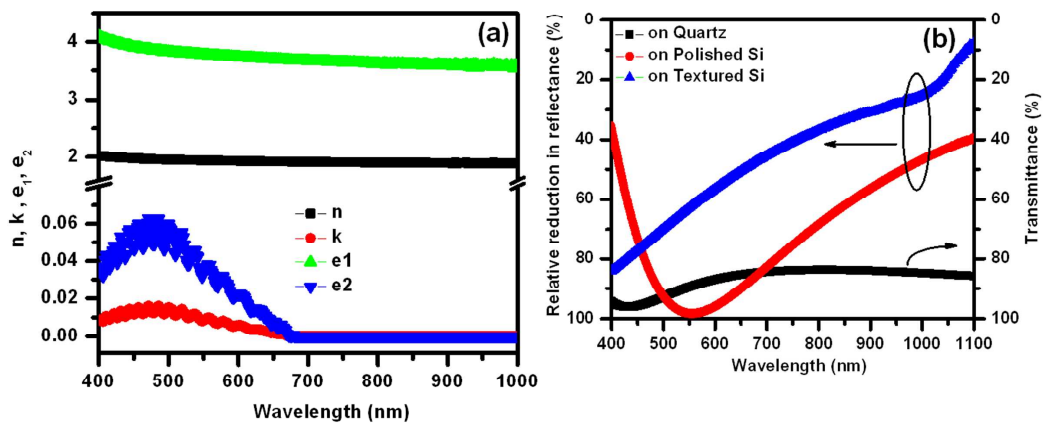


Figure 3: (a) Optical constants (n , k) and dielectric constants (e_1 , e_2); (b) relative reduction in reflectance values for a -BTO thin-film deposited on polished Si substrate & textured Si substrate, and transmittance value for a -BTO thin-film deposited on quartz substrate.

Figure 4

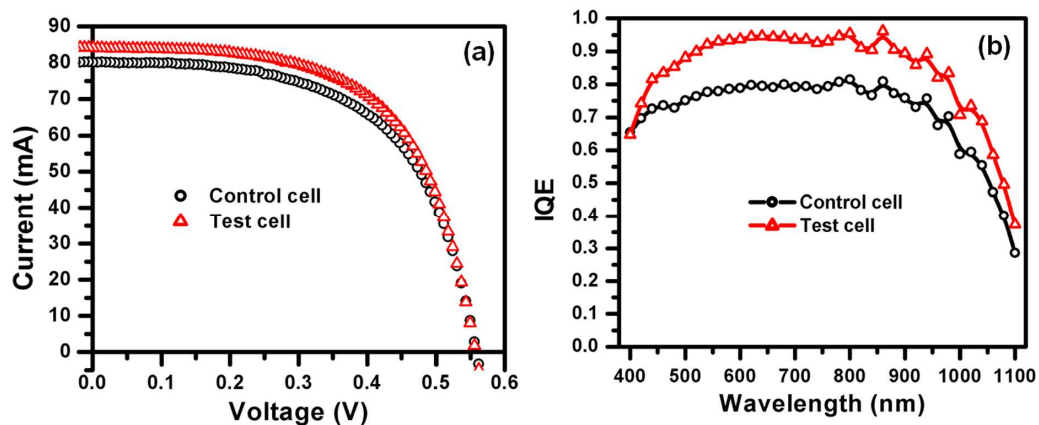


Figure 4: (a) Illuminated I-V characteristics; (b) Internal quantum efficiency (IQE) of control and test Si solar cell with and without α -BTO coating, respectively.